

Electrochemical preparation method of titanium dioxide on FTO

F. Rahal^{a,b}, A. Kamarchou^c, A. Berchi^a, D. Abdi^a, I. Kemerchou^{d,*}

^aLaboratory of Energy and electrochemistry of solid Process Engineering U.F.A. University of Sétif, Algeria

^bDepartment of Chemistry, Faculty of Science, Mouloud Mammeri University of Tizi-Ouzou, 15000, Algeria

^cLaboratory of pollution and waste treatment , University Kasdi merbah Ouargla, Ouargla 30000, Algeria

^dDepartment of Mechanical engineering, Faculty of Applied Science, University of Ouargla, 3000, Algeria

Cathodic electrodeposition of aqueous peroxo-titanium complex solution on fluorine doped tin dioxide (FTO) covered glass produced nanocrystalline amorphous and crystalline titanium dioxide. X-rays were used to examine the surface structures, which shows that heat treatment made a gradual crystallization of the deposits to the anatase form meanwhile the non-heated deposits present amorphous phase. Atomic force microscopy (AFM) and scanning electron microscopy (SEM) and atomic force microscopy (AFM) permit to investigate the morphological aspect of the deposits, which display a good adherence and a nanoparticulate grain size. The UV-Visible spectroscopic investigation technique reveals the better transparency aspect of the annealed films than the non-heated deposits. Ac impedance spectroscopy confirms the electrical conductivity of both deposits with more important activity for the non-heated deposits.

(Received June 26, 2022; Accepted September 15, 2022)

Keywords : Thin film, Electrochemical synthesis, Photoelectrochemical, Titanium dioxide

1. Introduction

Due to their remarkable structural, chemical, photochemical, optical, and electronic capabilities, scientific research has focused on nanostructured semiconductor materials. Due to its vital uses in environmental cleanup, photocatalysis, hydrophilic coating, and gas sensors, one of the most researched oxide materials is nanocrystalline titanium dioxide (TiO₂). [1-4]. Furthermore, a dye-sensitized solar cell DSSC was considered a really appealing application of TiO₂ [5-7]. The process of preparation can be crucial in creating an appropriate geometrical surface. most research studies have used the sol-gel method of preparation [8-10], hydrothermal [11], chemical vapor deposition [12,13], and electrodeposition [14-16], technology for depositing TiO₂ thin films from aqueous solution that is both convenient and adaptable. This technique has distinct advantages over other techniques due to uniformity, strict control of film thickness, deposition rate, and composition, careful regulation of reaction parameters such as solution concentration, and ease of adaptation to conformal deposition on substrates of complicated shape and geometry.

The aim of this paper is the preparation of crystalline and amorphous titanium dioxide films on FTO by electrodeposition, characterization of deposits by different techniques and comparison study between the amorphous and crystalline films. In more detail, the main objectives are: (1) to optimize the conditions of cathodic electrodeposition of TiO₂ coating then to elaborate them from aqueous solution on FTO using the voltamperometric cyclic as technique. (2) to investigate comparatively the structural characterization by XRD of such films, their morphological aspect by SEM and AFM and spectroscopic behavior by UV-Visible . and to give also the electrochemical impedance characteristics of both amorphous and crystalline deposits..

* Corresponding author:kemerchou.imad@univ-ouargla.dz
<https://doi.org/10.15251/JOR.2022.185.661>

2. Experimental details

2.1 Materials synthesis

In a tiny three-electrode cell, all deposits were made on optically transparent fluorine-tin-oxide coated glass plates (FTO, 20Ω/square; sample area in the 1.5 cm² range) were used as cathodic substrates.

Pt plate (20×10×1 mm) as the counter electrode and the Ag/AgCl_{sat} as a reference electrode; a Voltalab 340 potentiostat was employed. The FTO substrates were washed in acetone, propanol, and water for 5 minutes each before being used for film deposition. the substrate was etched in HNO₃ 45% for 2 minutes.

From an aqueous peroxy-titanium solution, titanium dioxide sheets were cathodically electrodeposited. The deposition bath mixed in a ratio KNO₃:TiOSO₄: H₂O₂=1:0.2:0.3 and an amount of HNO₃ to adjust the pH at 1.4; the bath temperature was maintained at 20°C range. The electrodeposition of cathodic metals was carried out between 0 mV and -1.4 mV (versus Ag/AgCl_{sat}) which led to the formation of TiO(OH)₂.xH₂O gel film on FTO. Following that, certain films were heated in air for 1 hour at 450°C to produce crystalline titanium dioxide thin films [8].

2.2. Thin films characterization

The crystallization behavior of the fresh and heat-treated electrodeposited titanium dioxide films was analyzed at room temperature by X-ray diffraction (XRD) using a PHILIPS X'PERT diffractometer with Cu Kα radiation and a 2θ scan rate of 0.01°/s. The surface morphological features of the films were observed using an LEO 982 scanning electron microscope (SEM). Images of the films were obtained using atomic force microscopic AFM and the scans were made on 1μm * 1μm areas of the films. Optical studies were obtained with UNICAM300 UV-Visible spectrophotometer in the UV-Visible range (200-1100nm).

The Ac impedance measurements were performed with standard three electrode system comprising electrodeposited titanium dioxide thin films on FTO as a working electrode, Pt as a counter electrode and Ag/AgCl_{sat} as a reference electrode. A 0.1M potassium sulfate solution was used as an electrolyte.

3. Results and discussion

3.1 Structural study

The X-ray diffraction (XRD) of the film of titanium dioxide as deposited and annealed at 450°C is shown in Figure 1(a). Pattern a and b in Figure 1(b) shows the characteristics peaks of the as deposited film and the film heated at 450°C for 1 hour in air. The film as deposited was found to be amorphous, as indicated by the absence of any diffraction peaks, such results have been observed by [16, 17], a faint broad peak at about 2θ=25 was observed. The heat-treated film at 450°C confirms the formation of an anatase structure of TiO₂, the sharp peak detected at 25.77 can be attributed to the anatase phase the same as for [18-20].

The average crystallite sizes of titanium dioxide deposits were estimated from the X-ray line broadening analysis by the Debye-Sherrer's equation ($D = \frac{0.9\lambda}{\beta \cos\theta}$) where: θ is the Bragg angle, λ=1.542Å is the wavelength of the X-ray radiation and β is full width at half maximum (FWHM). Calculation based on the peak at 2θ=25.775 gave a value of 4.9 nm.

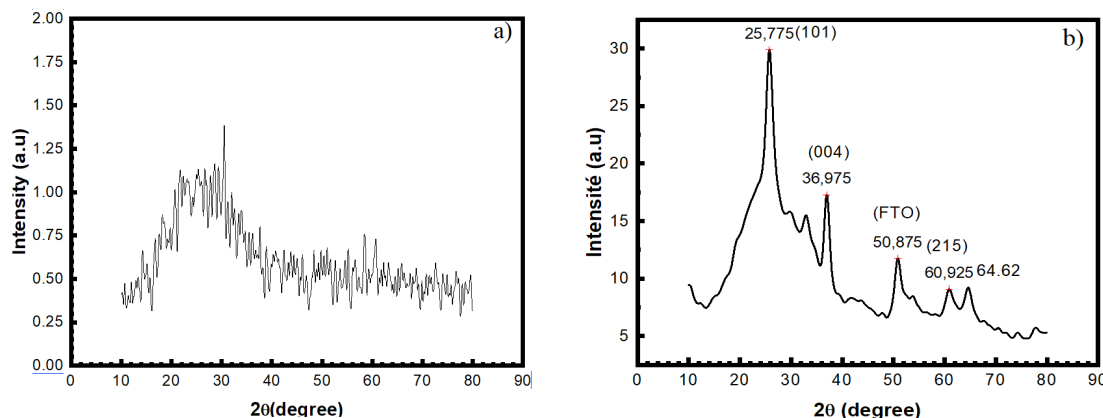
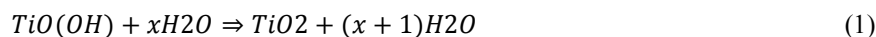


Fig. 1. X-ray diffraction (a,b) shows the characteristics peaks of the as deposited film.

3.2. Surface morphology

SEM images of as-deposited Figure 2(a) and heat-treated (450°C for 1 hour) materials are shown in Figure 2(b). It shows distinguished spherical morphology and confirms the formation of nanoparticulate and nanoporous films. The as deposited film was quite homogenous, it indicates clearly the particles to be roughly spherical and it shows areas richer in crystallites. On heat-treated titanium dioxide films, some fractures were discovered, which were attributed to film dehydration when subjected to heat treatment in accordance with the reaction.



They are likely similar to those produced by [21, 22]. Our deposits' surface morphology and topographic relief are investigated using the AFM method. Figures 3(a and b), the AFM top-view of two dimensional surface plots thin films, as deposited and annealed TiO_2 at 450°C for 1 hour, respectively. The fundamental variations between the two deposits may be seen in the surface morphology and roughness of the two films. A close analysis of the photos reveals that at 450°C heat treatment alters the surface topography. The AFM image of as-deposited titanium dioxide Figure 3(a) shows that a rough surface has formed. the mean square roughness value is 8.81 nm. The appearance of the AFM image of annealed film (Figure 3(b) seems to be quite similar to as deposited film, the mean square roughness value is decreased (6.79 nm), and this is probably due to the formation of aggregates of the particles by heat treatment, such observations are in agreement with our SEM pictures and XRD calculation peak size and they are in accordance with previous studies [22, 23].

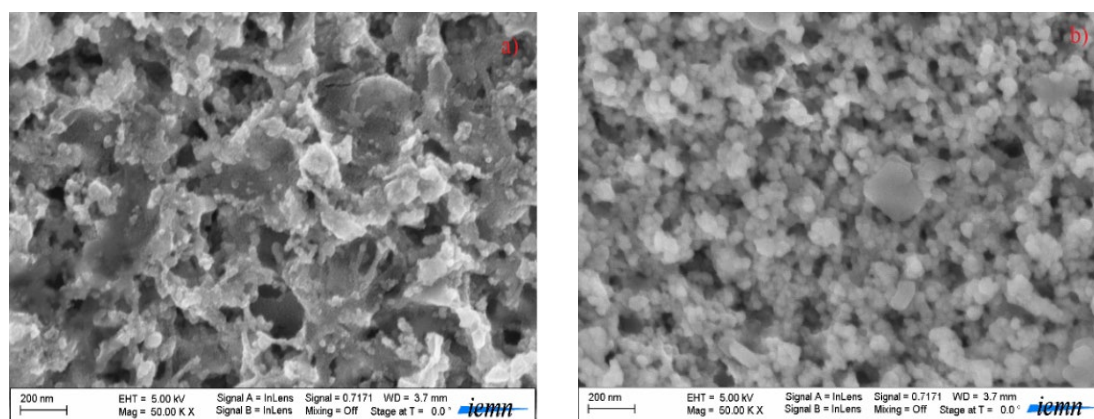


Fig. 2. (a,b) shows distinguished spherical morphology and confirms the formation of nanoparticulate and nanoporous films.

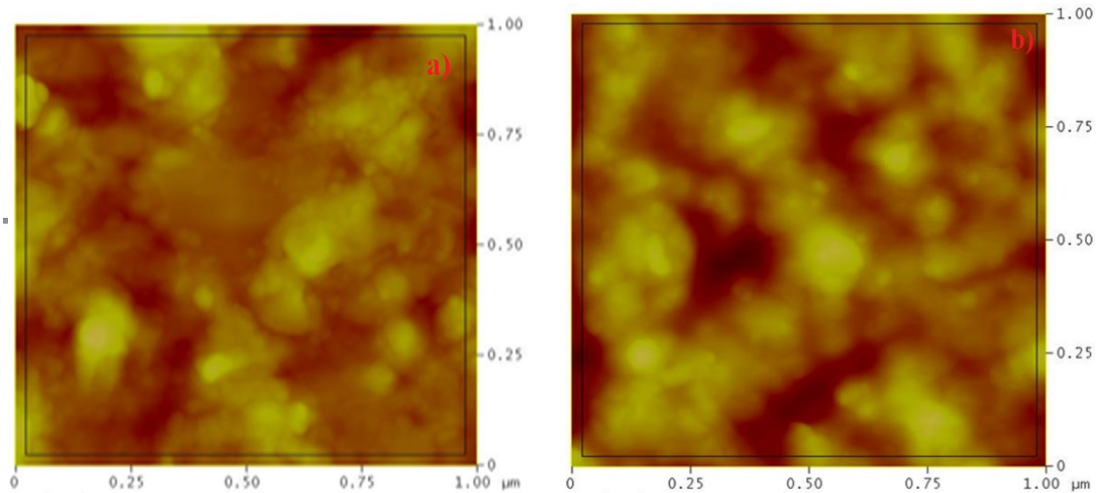


Fig. 3. (a,b) AFM image of as deposited titanium dioxide.

3.3. Optical properties

Figure 4 shows variation of optical absorption and transmittance with wavelength for the films of titanium dioxide as deposited and heat treated at 450°C for 1 hour. The FTO/glass as used as the reference. The optical absorption spectrum Figure 4(a) of titanium dioxide film as deposited on FTO showed the highly absorbent in the UV domain and a sharp increase in absorption below 350 nanometer wavelengths. The absorption spectrum of the titanium dioxide heat treated shows a similar route but less absorbance in the region of visible which is probably related to the difference morphology of both films. Such behavior has been reported by [16, 23].

Optical transmission of the titanium dioxide films on FTO as deposited and heat treated in the 200 to 1100 nm wavelength range are shown in Figure 4(b). In the UV region, transmittance for as deposited films and heat treated is similar and approaches to zero for the two. At about 350 nm the transmittance increase quickly for both films and approaches to 50% for the film as deposited and 70% for the heat treated likely to [24].

The difference of transmittance between the titanium dioxide as deposited and heat treated in the 350-1100 nm range was attributed to the difference in their film morphology as seen in the SEM images and AFM micrographs. This material has a high UV absorption and a high visible transmittance, let us to propose the employment of these kinds of films as a filter UV ray.

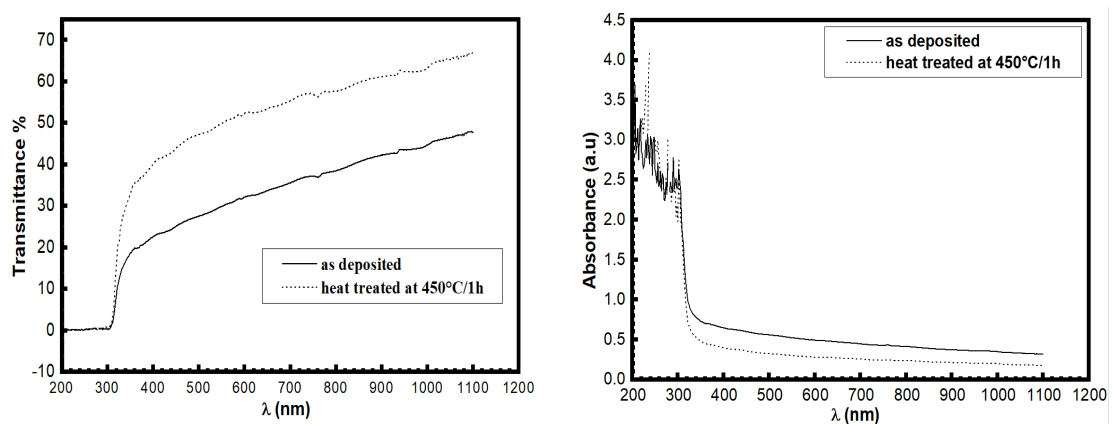


Fig. 4. (a, b) shows variation of optical absorption and transmittance with wavelength for the films of titanium dioxide as deposited and heat treated at 450°C for 1 hour.

3. 4 Electrochemical and photoelectrochemical characterization

The electrochemical characterization of titanium dioxide thin films on FTO as deposited (crystalline), and sintered at 450 °C for one hour in the air (amorphous) were carried out by fast scan rate (100 mV/s) cyclic voltamperometry experiment in order to establish the electrochemically active surface area of the titanium dioxide electrode in 0.1 M K₂SO₄ solutions (Figure 5 (a,b)). The cyclic voltamperograms present no significant currents at positive potentials ca. -0.2 V versus Ag/AgCl as expected for an n-type semiconductor [17]. At potentials more negative than ca. -0.2 V versus Ag/AgCl, both a cathodic peak and an ill-defined anodic hump or peak are observed, the former corresponding to the reduction of Ti(4) species at the surface in contact with the electrolyte to Ti(3), and the latter to the re-oxidation process obtained during the positive potential scan of surface Ti(3) species giving rise to a couple of conjugate cathodic and anodic peaks, characterised by an irreversibility system. In other hand we can observe that as deposited titanium film produces higher current values than the heated deposit in the potential range between -0.5 and -1.5. The current of the as deposited film is approximately 15 times higher than that corresponding to the heated film, which must be attributed to the high conductivity of the OH⁻ of the as deposited film TiO(OH)₂ on one hand, and to the decrease of the active surface site of heated thin film on the other hand. In the potential range studied, the hydrogen adsorption-desorption process also takes place.

Ac impedance spectroscopy is a powerful technique to determine the kinetic parameters of the electrode process. In this part, we have combined it with illumination process. The ac impedance spectrums at the dark and under illumination of titanium dioxide thin films on FTO as deposited and heat treated are illustrated in Figure 6(a) and Figure 6(b) respectively. All impedance plots were determined at -300 mV within a frequency range between 100 kHz and 10 MHz with a decreasing scanning frequency order. As can be seen, both the Nyquist plots are characteristic of one semicircle which represents an electrochemistry controlled process, related to the charge transfer through the electrode/electrolyte interface. From the Nyquist plots, it can be found that the size of semicircle of titanium as deposited at the dark is smaller than the titanium dioxide heated at 450 °C, therefore the charge transfer resistance of the latter is lower than the former, so it implies that the titanium oxide as deposited is more conductive than the titanium dioxide deposited and heat treated at 450 °C for one hour which are in good agreement with previous results [25-27]

The photoelectrochemical study of two films using the impedance plots in the dark and under UV illumination were carried out in a three electrode cell equipped with a flat quartz window opposite the working electrode (exposed front face electrode area of 1 cm²). An Ag/AgCl as the reference electrode and a Pt plate rectangular as the counter electrode. Fig. 6. a. and Fig. 6. b. show Nyquist plots obtained at -300 mV within a frequency range between 100 KHz and 10 mHz with a decreasing scanning frequency order at the dark then under illumination UV ($\lambda=365\text{nm}$). As can be seen from Figure 6. All the plots after illumination UV indicate semicircles like the plots at the dark. It is observed that the semicircle diameter of titanium dioxide not annealed under the illumination is shorter than that same film at the dark, implying the charge transfer R_{ct} of the former (219.6 K Ω .cm²) is smaller than the latter (305.8 K Ω .cm²). This result reveals that the charge transfer rate under illumination is higher than that at the dark for the amorphous form of the film. For the crystalline titanium dioxide obtained after annealing, we can observe the same phenomenon, the transfer rate of charge under illumination ($R_{ct} = 427.3 \text{ K}\Omega$.cm²) is higher than that at the dark ($R_{ct} = 1414 \text{ K}\Omega$.cm²)

R_{ic} values obtained from the fitting of the equivalent circuit, for two films at the dark and under illumination UV ($\lambda=365\text{nm}$) are presented in table 1.

Table 1. values obtained from the fitting of the equivalent circuit.

Electrode	R_{ic} (K Ω .cm ²)	Electrode	R_{ic} (K Ω .cm ²)
(a)	305.8	(c)	1414
(b)	219.6	(d)	427.3

From the spectroscopic impedance results, we can say that both films, as-deposited and heated present important photogenerated currents under illumination and inform us on the possibility to use the crystallized and non-crystallized film. On the other hand, The surface of the non-crystallized film is more active, because of the abundance of OH, it may be employed as a photocatalytic material electrode, which appears to play a key role in the pollutant degradation pathways and can contribute to the radical OH produced by hole trapping, and It would be extremely beneficial, as the elaboration of non-crystallized films did not necessitate a higher temperature [28-31].

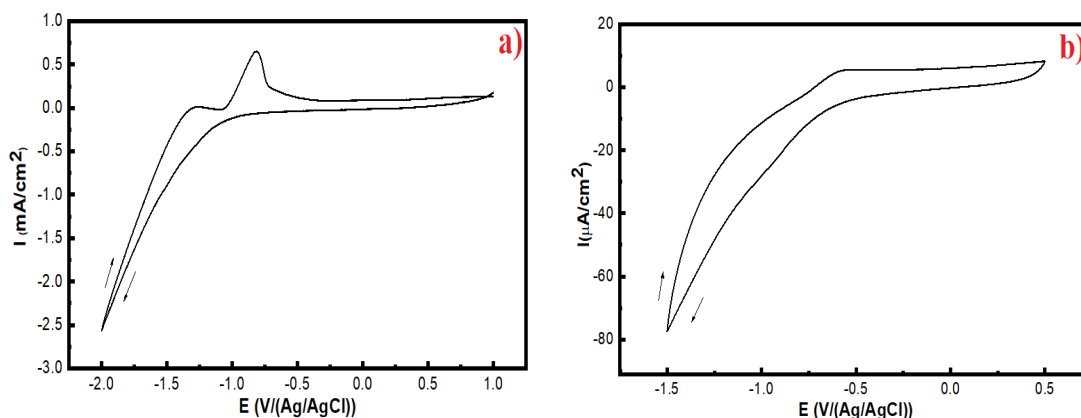


Fig. 5. (a,b) Cyclic voltamperograms presents no significant currents at positive potentials ca. -0.2 V versus Ag/AgCl as expected for an n-type semi-conductor.

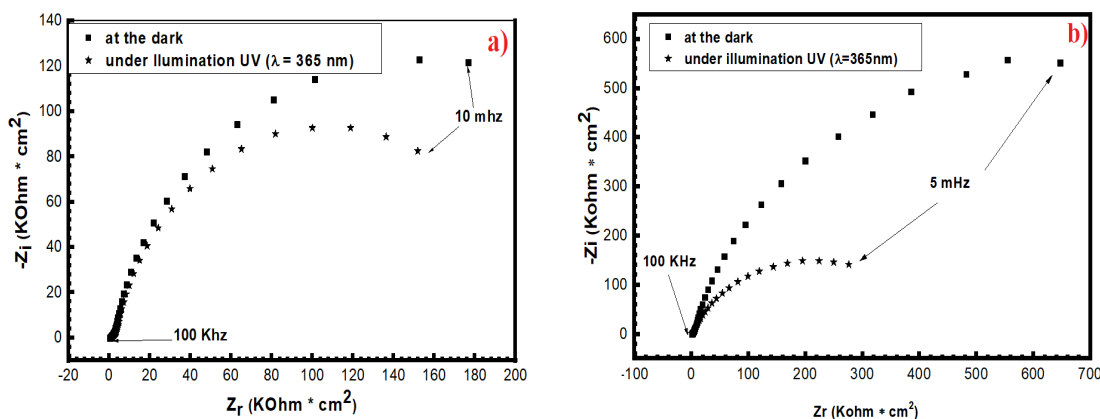


Fig. 6. a Nyquist plots for titanium dioxide on FTO as deposited, heated at 450°C for 1h at -300 mV in 0.1 M K_2SO_4 , at the dark and under the illumination.

Fig. 6. b Nyquist plots for titanium dioxide on FTO, heated at 450°C for 1h at -300 mV in 0.1 M K_2SO_4 , at the dark and under the illumination.

4. Conclusions

The Electrodeposition route has been used to prepare nanosized titanium dioxide on FTO from peroxy-titanium solution. The potential window for their deposition lies between 0 and -1.4 mV. The X-ray diffraction (XRD) show that the film as deposited was amorphous and the film heat treated present a crystalline anatase structure. The scanning electron microscopy (SEM), and atomic force microscopy (AFM) show the homogeneity and little roughness of the films. The UV-Visible analysis shows a great similarity in the spectroscopy behaviour between the annealed and non-annealed films. The great absorbance in UV domain and the great transmittance in the visible

range of such films promote them to be used as a filter UV ray. Results of spectroscopic impedance combined with illumination depict the photoelectrical activity of both films.

Acknowledgments

This work was partly supported by Laboratory of pollution and waste treatment Ouargla. Uv visible data in this work supported by Lab. VTRS, Faculty of Technology, Univ. El-Oued,

References

- [1] Z. S. Jiajia Tao, Y.Cheng, M. Zhang, J.Lv, SH.Shi, G.he, X. C, Xishun Jiang, X. Wang, Zh. Wang, Ze. Gong. Nature,7,9, (2017); [10.1038/s41598-017-05645-x](https://doi.org/10.1038/s41598-017-05645-x)
- [2] S. S. Maryam Zare, A Shafiekhani, S. Kulesza, and Ş. T. a. M. Bramowicz, Nature, 8,11, (2018); [10.1038/s41598-018-29247-3](https://doi.org/10.1038/s41598-018-29247-3)
- [3] N. T. S. Roy, P. K. Sahu, J. P. Kar, Materials in Electronics, 30,15928–15934, (2019); [10.1007/s10854-019-01944-3](https://doi.org/10.1007/s10854-019-01944-3)
- [4] C. K. M. Nagalakshmi, N. Anusuya, C. Brundha, M. Jothi Basu and S. Karuppuchamy, Mater Electron, 28, 15915–15920, (2017); [https://doi.org/10.1007/s10854-017-7487-](https://doi.org/10.1007/s10854-017-7487-7)
- [5] Q. Z. Nuoxin Xu, Hui Yang, Yuting Xia and Yongchang Jiang, Nature, 7,9,(2017); <http://dx.doi.org/10.1038/srep43970>
- [6] P.Venkatachalam, K.Anandalakshmi, Optical Materials,109,5, (2020); <https://doi.org/10.1016/j.optmat.2020.110335>
- [7] M. T. N. Nesrine Amor, Michal Petru, Aamir Mahmood and A. Ismail, Nature,11,13, (2021); <https://doi.org/10.1038/s41598-021-93108-9>
- [8] T. S. Makoto Hayashi, Masashi Imamura, Shunsuke Fujibayashi, K. G. Seiji Yamaguchi, Bungo Otsuki1, Toshiyuki Kawai, Yaichiro Okuzu and S. Matsuda, Nature,11,9, (2021); <https://doi.org/10.1038/s41598-021-95572-9>
- [9] R. I. M. Dimitrov, N. Velinov, J. Henych, M. Slušná, V. Štengl, J. Tolasz, I. Mitov, T. Tsoncheva, Nano-Structures & Nano-Objects,7,56–63, (2016); <http://dx.doi.org/10.1016/j.nanoso.2016.06.001>
- [10] K. M. S. Shreesha Bhat, Prasad Kumar, S. M. Dharmaprakash and K. Byrappa, J Mater Sci: Mater Electron, 9, (2017); [10.1007/s10854-017-8011-2](https://doi.org/10.1007/s10854-017-8011-2)
- [11] J. S. Aschariya Prathan, Tao Wang, Chawalit Bhoomanee, and A. G. a. D. W. Pipat Ruankham, Nature,10,11, (2020); <https://doi.org/10.1038/s41598-020-64510-6>
- [12] R. N. Muhammad Ali Ehsan, Vickie McKee, Abdul Rehman, Abbas Saeed Hakeem and M. Mazhar, Journal of Materials Science: Materials in Electronics,30, 1411–1424, (2018); <https://doi.org/10.1007/s10854-018-0411-4>
- [13] N. KARTHI, K. A. RAMESHKUMAR, P. MAADESWARAN, Journal of Ovonic Research, 17, 1, 73 - 80, (2021); https://chalcogen.ro/73_KarthiN.pdf
- [14] K. A. B. A. T. R. R. C. R. Shyniya, Journal of Materials Science: Materials in Electronics, 29, 16270–16281, (2018); <https://doi.org/10.1007/s10854-018-9716-6>
- [15] X. Zaichun Liu, Sh. Zhang, J.ang, Q.Huang, N. Yu, Y.usong Zhu, L. Fu, and Y. C. a. Faxing Wang, NPG Asia Materials,12,1-21(2019); <https://doi.org/10.1038/s41427-019-0112-3>
- [16] C. Tian,Nature,10,9, (2020); [https://doi.org/10.1038/s41598-020-64976-](https://doi.org/10.1038/s41598-020-64976-7)
- [17] Y. X. T. S. Kunihiko Kato, Nature, 9, (20 March 2019); <https://doi.org/10.1038/s41598-019-41465-x>
- [18] J.-J. C. Wei-Kang Wang, Xing Zhang, Yu-Xi Huang, Wen-Wei Li and Han-Qing Yu, Nature 2016,6,10; [10.1038/srep20491](https://doi.org/10.1038/srep20491)
- [19] K. V. A. K. Cilaveni Goutham, Sai Santosh Kumar Raavi, and S. Asthana, Journal of Materiomics,8,18-29, (2021); <https://doi.org/10.1016/j.jmat.2021.06.003>
- [20] K. S. Jaspal Singh, Biswarup Satpati and S.Mohapatra, Optik,188,270–276, (2019); <https://doi.org/10.1016/j.ijleo.2019.05.053>

- [21] Feyza Güzelçimen , Vacuum, 182,109766,(2020); <https://doi.org/10.1016/j.vacuum.2020.109766>
- [22] O. T. Najoua Bouzakher-Ghomrasni , Jocelyne Leroy , Nicolas Feltin, and F. T. a. C. Chivas-Jolye, Talanta, 234, 122619, (2021); <https://doi.org/10.1016/j.talanta.2021.122619>
- [23] A. L. A. E. A. Oili M. E. Ylivaara ; Mechanical and optical properties of as-grown and thermally annealed titanium dioxide from titanium tetrachloride and water by atomic layer deposition. Thin Solid Films 2021,732,138758; <https://doi.org/10.1016/j.tsf.2021.138758>
- [24] A. M. A. Ibrahim Morad, A.F. Mansour, M.H. Wasfy , M.M. El-Desoky, Physica B: Physics of Condensed Matter,597,9, 412415, (2020); <https://doi.org/10.1016/j.physb.2020.412415>
- [25] Z. H. Jie Ding, Jihao Zhu, Shengzhong Kou, X. Zhang and and H. Yang, Nature, 5, 17773, (2015); <https://dx.doi.org/10.1038%2Fsrep17773>
- [26] D. G. G. Amanda Jo Zimmerman , V. Montero Campos , S. K. D. David C. Weindorf , Sharon Ulate Chacón , Gautier Landrot , and N. G. G. F. a. M. G. Siebecker, Environmental Advances, 3, 100036, (2021); <https://doi.org/10.1016/j.envadv.2021.100036>
- [27] A. A. S. Galina A. Zenkovets , Vladimir Yu and Gavrilov, Materials Research Bulletin, 145, 111538, (2022); <http://doi.org/10.1016/j.materresbull.2021.111538>
- [28] X. L. Yu Du, Xiang Ren, H.Wang, D.Wu, H. Ma, and D. F. a. QinWei, Analyst, 5,1858-1864, (2 Mar 2020); [10.1039/c9an02288k](https://doi.org/10.1039/c9an02288k)
- [29] P. S. Qian S, Zhang Y, Wang P, Bai Y, Lai B, J Environ Sci (China),100,99-109, (2020); <https://doi.org/10.1016/j.jes.2020.06.039>
- [30] X. X. Jie Z, Huan Y, Youkang H, Zhiyao Z, Environ Technol, 2,193-205, (Jan 2021); <https://doi.org/10.1080/09593330.2019.1625955>
- [31] K. B. Park YK, Kim SC, You CS, Choi J, Park J, Lee H, Jung SC, Environmental Research, 195, 110899, (Apr 2021); <https://doi.org/10.1016/j.envres.2021.110899>